Journal of Southeast University (English Edition) Vol. 25, No. 3, pp. 289 – 293 Sept. 2009 ISSN 1003—7985

Improved absorbing boundary condition based on linear interpolation for ADI-FDTD method

Zhao Jianing

(National Mobile Communications Research Laboratory, Southeast University, Nanjing 210096, China)

Abstract: With the linear interpolation method, an improved absorbing boundary condition (ABC) is introduced and derived, which is suitable for the alternating-direction-implicit finite-difference time-domain (ADI-FDTD) method. The reflection of the ABC caused by both the truncated error and the phase velocity error is analyzed. Based on the phase velocity estimation and the nonuniform cell, two methods are studied and then adopted to improve the performance of the ABC. A calculation case of a rectangular waveguide which is a typical dispersive transmission line is carried out using the ADI-FDTD method with the improved ABC for evaluation. According to the calculated case, the comparison is given between the reflection coefficients of the ABC with and without the velocity estimation and also the comparison between the reflection coefficients of the ABC with and without the nonuniform processing. The reflection variation of the ABC under different time steps is also analyzed and the acceptable worsening will not obscure the improvement on the absorption. Numerical results obviously show that efficient improvement on the absorbing performance of the ABC is achieved based on these methods for the ADI-FDTD.

Key words: alternating-direction-implicit finite-difference time-domain (ADI-FDTD) method; absorbing boundary condition (ABC); linear interpolation; phase velocity; nonuniform cell

The finite-difference time-domain (FDTD) method is widely used for solving various kinds of electromagnetic problems[1-2]. Recently, ADI-FDTD methods[3-4] were developed to remove the Courant-Friedich-Lecy (CFL) stability condition. Therefore, the time step used in the ADI-FDTD method is no longer limited to the stability conditions but by the modeling accuracy of the algorithm.

When the FDTD method is used for open structure problems, truncated boundary conditions are required to convert the unlimited physical space to the limited calculable space. Generally, two kinds of truncated boundary conditions are used in the FDTD method. One is the ABC based on the traveling wave equations[5-7] and the other one is the perfect matched layer (PML) based on the absorbing media[8-10]. The ABC requires much less computation and memory but may introduce greater reflection than the PML under small CFL factor conditions. However, it is demonstrated that the ABC and the PML have almost the same level of accuracy for large CFL factors because of the numerical dispersion[11]. Therefore, the investigation on the implemention and improvement of the ABC is significant for the ADI-FDTD method especially under the large CFL factor conditions.

Using the ADI-FDTD method reduces the implicit iteration complexity of the field equations by forming a tridiagonal matrix. In order to take advantage of such characteristics of the ADI-FDTD method, the linear interpolation method is used in this paper for the ABC field estimation, which indicates that the first-order ABC will be used. The methods in this paper are developed to improve the performance of the first-order ABC.

1 Construction and Analysis of the ABC

1.1 Construction of the ABC

For a traveling plane wave along a $+z$ direction in a lossless isotropic medium, the electric field can be expressed as

$$\boldsymbol{E}(x, y, z, t) = \boldsymbol{E}_0(x, y) f\left(t - \frac{z}{v}\right) \tag{1}$$

where $v = c/\cos\theta$ is the phase velocity of the plane wave along the z-axis; c is the light speed in the medium, and θ is the incident angle of the plane wave.

For simplicity, let $x = x_0$ and $y = y_0$ for fixed transverse coordinates. Then Eq. (1) can be rewritten as

$$\boldsymbol{E}(z, t) = \boldsymbol{E}_0 f\left(t - \frac{z}{v}\right) \tag{2}$$

The field on the absorbing boundary ($z = z_0$) can be expressed as

$$\boldsymbol{E}(z_0, t) = \boldsymbol{E}_0 f\left(t - \frac{z_0}{v}\right) = \boldsymbol{E}(z_0 - \Delta z, t - \xi\Delta t) \tag{3}$$

where $\xi = \Delta z/(v\Delta t)$; Δt is the time increment, and Δz is the space increment in the z-direction.

Denote the field on the absorbing boundary with $\boldsymbol{E}_a(t) = \boldsymbol{E}(z_0, t)$ and the inside field at the first node the boundary with $\boldsymbol{E}_{i1}(t) = \boldsymbol{E}(z_0 - \Delta z, t)$. According to Eq. (3), the following relationship can be obtained,

$$\boldsymbol{E}_a(t) = \boldsymbol{E}_{i1}(t - \xi\Delta t) \tag{4}$$

Eq. (4) implies that the field on the absorbing boundary can be determined by the inside field at the first node with a time delay $\xi\Delta t$ ahead of the current time t; i.e., the absorbing boundary condition is equivalent to the estimation of $\boldsymbol{E}_{i1}(t - \xi\Delta t)$. Generally, ξ is a decimal.

With the relationship in Eq. (4), the straightforward method to estimate the value of $\boldsymbol{E}_i(t - \xi\Delta t)$ is the linear interpo-

Received 2008-12-08.

Biography: Zhao Jianing (1976—), female, doctor, lecturer, jnzhao@seu.edu.cn.

Foundation items: The National Natural Science Foundation of China (No. 60702027), the Free Research Fund of the National Mobile Communications Research Laboratory of Southeast University (No. 2008B07), the National Basic Research Program of China (973 Program) (No. 2007CB310603).

Citation: Zhao Jianing. Improved absorbing boundary condition based on linear interpolation for ADI-FDTD method[J]. Journal of Southeast University (English Edition), 2009, 25(3): 289 – 293.

lation method,

$$\boldsymbol{E}_{\mathrm{a}}(t) = \boldsymbol{E}_{i1}(t-\xi\Delta t) \approx (1-2\xi)\boldsymbol{E}_{i1}(t) + 2\xi\boldsymbol{E}_{i1}\left(t-\frac{\Delta t}{2}\right) \quad (5)$$

Eq. (5) can be rearranged for the ADI-FDTD iteration as follows:

First procedure

$$\left.\begin{aligned} -\alpha_{i,j,k}E_y\Big|_{i,j,k-1}^{n+1/2} + \beta_{i,j,k}E_y\Big|_{i,j,k}^{n+1/2} &= 2\xi E_y\Big|_{i,j,k-1}^{n} \\ E_y\Big|_{i,j,k}^{n+1} &= \alpha_{i,j,k}E_y\Big|_{i,j,k-1}^{n+1} + 2\xi E_y\Big|_{i,j,k-1}^{n+1/2} \end{aligned}\right\} \quad (6a)$$

Second procedure

$$\left.\begin{aligned} E_x\Big|_{i,j,k}^{n+1/2} &= \alpha_{i,j,k}E_x\Big|_{i,j,k-1}^{n+1/2} + 2\xi E_x\Big|_{i,j,k-1}^{n} \\ -\alpha_{i,j,k}E_x\Big|_{i,j,k-1}^{n+1} + \beta_{i,j,k}E_x\Big|_{i,j,k}^{n+1} &= 2\xi E_x\Big|_{i,j,k-1}^{n+1/2} \end{aligned}\right\} \quad (6b)$$

where $\alpha_{i,j,k} = 1-2\xi$ and $\beta_{i,j,k} = 1$.

Actually, the ABC (5) is similar to the results shown in Ref. [6]. However, the derivation is based on the linear interpolation and not on the discrete processing in Ref. [6]. If $\xi < 1$, the coefficients of the ADI tri-diagonal will satisfy $|\beta| > |\alpha| + |\gamma|$ and the ADI tri-diagonal can be solved without any difficulties[4].

1.2 Error analysis of the ABC

However, it is very difficult to obtain the exact phase velocity of the plane wave in advance. An inaccurate phase velocity will cause inadequately accurate results when using the ABC. The truncation of the expression of the field will also cause numerical errors. The error of the ABC, which includes the error introduced by the inaccurate phase velocity and the error introduced by the linear interpolation truncations, can be derived by virtue of a homochromous plane wave[2] as

$$\boldsymbol{E}_{i1}(t) = \mathrm{Re}\{\dot{\boldsymbol{E}}_{i10}\mathrm{e}^{\mathrm{j}\omega t}\} \quad (7)$$

The relative reflection power or the error power of the ABC under such conditions can be estimated by

$$P_{\mathrm{err}} \approx (\omega\Delta t)^2\left[\frac{(\omega\Delta t)^2(2\xi_0^2-\xi)^2}{16} + (\xi_0-\xi)^2\right] \quad (8)$$

where $\xi_0 = \Delta z/(v_0\Delta t)$, and v_0 is the actual phase velocity of the plane wave.

Furthermore, the phase velocity can be described by the incident angle of the plane wave as $v = c/\cos\theta$ and $v_0 = c/\cos\theta_0$, where v and θ are the estimated phase velocity and the incident angle respectively which are used in ABC (5), and θ_0 is the actual incident angle of the plane wave.

Fig. 1 shows the relationship between the logarithmic reflection coefficient and the actual incident angle of the plane wave under the conditions $f = 10$ GHz and $\Delta t = 4.7$ ps.

Obviously, the reflection increases significantly when the estimated phase velocity deviates from the actual value. Therefore, the estimation of the phase velocity is very important to ABC performance. Another indication is that the cell size which is relative to the truncated error also impacts the reflection of the ABC.

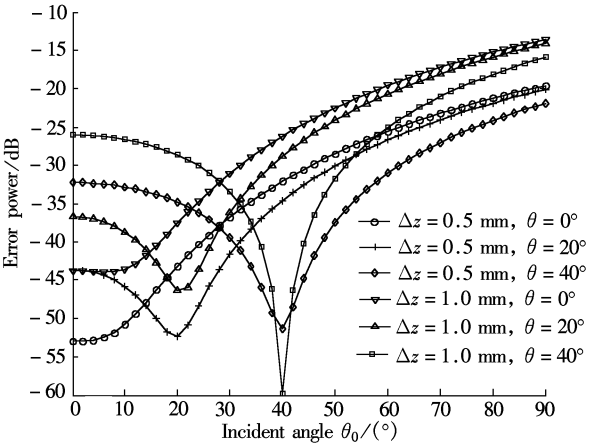

Fig. 1 Reflection coefficients of the ABC with different incident angles

2 Estimation of the Wave Velocity

According to the description above, if the actual phase velocity is used in the ABC (5), optimal absorbing performance can be obtained. For weak dispersion transmission lines, such as the TEM or quasi-TEM transmission lines, the phase velocity can be accurately calculated in advance. However, for strong dispersion transmission lines, such as the rectangular waveguide, the phase velocity used in Eq. (5) may affect the absorption performance.

In the previously reported ABCs, fixed phase velocity is used to solve the problems limited to weak dispersion transmission lines. For strong dispersion cases, high-order ABCs are often used to improve the absorption performance by selecting several different phase velocities in the construction of the ABCs. On the other hand, although these high-order ABCs have good performance, they are quite difficult to be adopted in the ADI-FDTD since the tri-diagonal matrix may be destroyed during the iteration. In this paper, the first-order ABCs with adaptive phase velocities will be used to take advantage of the tri-diagonal matrix and also have quite good reflection absorbing performance.

To reduce the reflection, an adaptive phase velocity estimation algorithm is developed.

According to Eq. (5), denote $\boldsymbol{E}_{i2}(t) = \boldsymbol{E}[t-(z_0-2\Delta z)/v]$, and then the phase velocity can be expressed as

$$v_1 = \frac{\Delta z}{\Delta t\xi_1} \approx \frac{2\Delta z}{\Delta t}\left|\frac{\boldsymbol{E}_{i2}(t-\Delta t) - \boldsymbol{E}_{i2}(t-\Delta t/2)}{\boldsymbol{E}_{i1}(t-\Delta t/2) - \boldsymbol{E}_{i2}(t-\Delta t/2)}\right| \quad (9)$$

Obviously, the phase velocity is a function of time t. Assuming that it varies very slowly with time and space, the phase velocity appearing in the ABC (5) can be approximately estimated by (9).

Again, a homochromous plane wave is used to calculate the numerical error. Then the electric field at $z = z_0 - \Delta z$ and $z = z_0 - 2\Delta z$ can be expressed as

$$\boldsymbol{E}_{i1}(t) = \boldsymbol{E}_{i0}\cos[\omega t - k(z_0-\Delta z)] = \mathrm{Re}\{\dot{\boldsymbol{E}}_{i1}\mathrm{e}^{\mathrm{j}\omega t}\} \quad (10)$$

$$\boldsymbol{E}_{i2}(t) = \boldsymbol{E}_{i0}\cos[\omega t - k(z_0-2\Delta z)] = \mathrm{Re}\{\dot{\boldsymbol{E}}_{i2}\mathrm{e}^{\mathrm{j}\omega t}\} \quad (11)$$

Substituting Eqs. (10) and (11) into Eq. (9), one can obtain

$$v_1 \approx \frac{2\Delta z}{\Delta t} \frac{\sin[\varphi_1 + (k\Delta z - \omega\Delta t/2)/2]\sin(\omega\Delta t/4)}{\sin\varphi_1 \sin(k\Delta z/2)} \tag{12}$$

where $\varphi_1 = \omega(t - \Delta t/2) - k(z_0 - \Delta z) + k\Delta z/2$.

In most cases, the cell size and the time step should be small enough to obtain sufficient numerical accuracy. Under such conditions, the values of $k\Delta z$ and $\omega\Delta t$ are less than 1. Therefore, Eq. (12) can be approximated as

$$v_1 \approx v + v\frac{k\Delta z - \omega\Delta t/2}{2\tan\varphi_1} \tag{13}$$

where $v = \omega/k$ is the actual phase velocity.

So the error of the estimation algorithm is

$$e = v_1 - v = v\frac{k\Delta z - \omega\Delta t/2}{2\tan\varphi_1} \tag{14}$$

From Eq. (14), it is clear that the numerical error is dependent on the space increment Δz, the time increment Δt and the phase φ_1. If $k\Delta z \ll 1$ and $\omega\Delta t \ll 1$, the phase φ_1 will be the main factor in the error. In order to reduce the error, the estimation will be carried out only when the value of $|\tan\varphi_1|$ is large enough. The value of $|\tan\varphi_1|$ can be calculated approximately by

$$K = |\tan\varphi_1| \approx \left|\frac{\boldsymbol{E}_{i1}(t - \Delta t/2) - \boldsymbol{E}_{i2}(t - \Delta t/2)}{\boldsymbol{E}_{i1}(t - \Delta t/2) + \boldsymbol{E}_{i2}(t - \Delta t/2)}\right| \tag{15}$$

With the assumption that the phase velocity varies with the time very slowly, only when K is greater than a threshold value, can the phase velocity be estimated and updated during the ADI-FDTD calculation using the ABC. Otherwise, the previous estimated velocity in the last iterative step can be used without change.

3 Nonuniform Cell

According to the reflection power in Eq. (8) and Fig. 1, the error of the ABC is also relevant to the cell size Δz. If both the simplicity and the accuracy need to be obtained during the numerical calculation, the nonuniform cell processing shown in Fig. 2 can be adopted; i. e., the cell size Δz can be much smaller near the absorbing boundary to reduce the reflection without increasing the total node number. The nonuniform cell processing is used in Ref. [4] covering the space needing to be investigated in detail but it does not include the space near the absorbing boundary.

Unlike the traditional FDTD method, the ADI-FDTD method is unconditionally stable. The space cell size can be set to a small enough value without adjusting the time step. Therefore, although Δz becomes smaller, no additional computation time is required compared with the uniform cell processing.

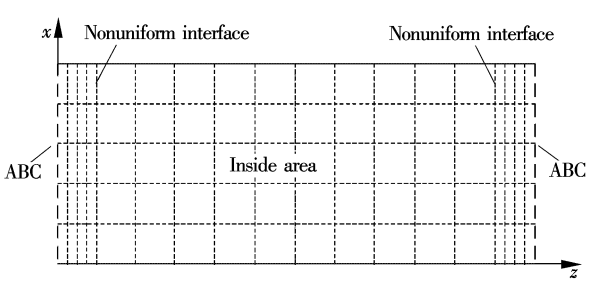

Fig. 2 Nonuniform cell processing used in the ABC in this paper

The decreased space step, directly used in Ref. [4] when calculating the fields on the nonuniform interface, does not describe the gradual change in the space step well. However, the nonuniform cell size can be processed by Eq. (16) which is the first procedure of the iteration step in the ADI-FDTD for example. This provides higher accuracy than the nonuniform processing in Ref. [4].

$$\alpha_{z1}(i,k)E_y\Big|_{i,k-1}^{n+1/2} + \beta_{z1}(i,k)E_y\Big|_{i,k}^{n+1/2} + \gamma_{z1}(i,k)E_y\Big|_{i,k+1}^{n+1/2} = \delta_{z1}(i,k) \tag{16}$$

where

$$\alpha_{z1}(i,k) = -\frac{1}{\mu\left(i,k-\frac{1}{2}\right)\left[\Delta z\left(k-\frac{1}{2}\right)\right]^2}$$

$$\gamma_{z1}(i,k) = -\frac{1}{\mu\left(i,k+\frac{1}{2}\right)\Delta z(k)\,\Delta z\left(k+\frac{1}{2}\right)}$$

$$\beta_{z1}(i,k) = \frac{2}{\Delta t}\left[\frac{2\varepsilon(i,k)}{\Delta t} + \frac{\sigma(i,k)}{2}\right] - \alpha_{z1}(i,k) - \gamma_{z1}(i,k)$$

$$\delta_{z1}(i,k) = \frac{2}{\Delta t}\left[\frac{2\varepsilon(i,k)}{\Delta t} - \frac{\sigma(i,k)}{2}\right]E_y\Big|_{i,k}^{n} + \frac{2}{\Delta t\Delta z(k)}\cdot \left(H_x\Big|_{i,k+1/2}^{n} - H_x\Big|_{i,k-1/2}^{n}\right) - \frac{2}{\Delta t\Delta x}\left(H_z\Big|_{i+1/2,k}^{n} - H_z\Big|_{i-1/2,k}^{n}\right)$$

$$\Delta z(j) = \begin{cases} \Delta z_1 & \text{inside } S \\ \dfrac{\Delta z_1 + \Delta z_2}{2} & \text{on } S \\ \Delta z_2 & \text{outside } S \end{cases}$$

S is the interface plane of the nonuniform cells shown in Fig. 2; Δz_1 and Δz_2 are the cell sizes inside and outside the interface plane S, respectively.

4 Numerical Simulation

In order to evaluate the ABC developed above, a rectangular waveguide problem is solved with the ADI-FDTD. The rectangular waveguide is a typical dispersive transmission line whose phase velocity significantly varies within its operation frequency band for the fundamental mode.

The simulation is carried out in an X-band rectangular waveguide with the ADI-FDTD method in 2D (TM_y) case. The differential Gauss pulse (17) is used as the excitation as

$$E_e(t) = \frac{t - t_0}{\tau}\exp\left[-\frac{4\pi(t - t_0)^2}{\tau^2}\right] \tag{17}$$

where $t_0 = 235$ ps and $\tau = 23.5$ ps. Since the purpose of this paper is to investigate the performance of the ABC; i. e., no discontinuity exists, hard excitation is used during the simulation for simplicity.

The observing point of the reflection is set at the position

10 grids away from the absorbing boundary. Up to 6 000 iterations are carried out to obtain the complete waveform which can be used to obtain the spectrum by the discrete Fourier transformation.

4.1 Uniform cell processing example

In this example, we use the following parameters: Δx = 1 mm, $\Delta z = 1$ mm, and $\Delta t = 4.7$ ps.

Fig. 3 provides the comparison of the reflection coefficients of the ABC with and without the velocity estimation. Relatively significant reflections can be observed if the fixed phase velocity is used in the ABCs. The error of the estimation in Eq. (14) is the function of the frequency. The value of the error is different when the value of K in Eq. (15) varies during the calculation. Therefore, the reflection of the ABC with velocity estimation appears to fluctuate over the frequency band in Fig. 3. However, it is obvious that the accurate velocity estimation will bring about an improvement of the reflection over the whole operation frequency band.

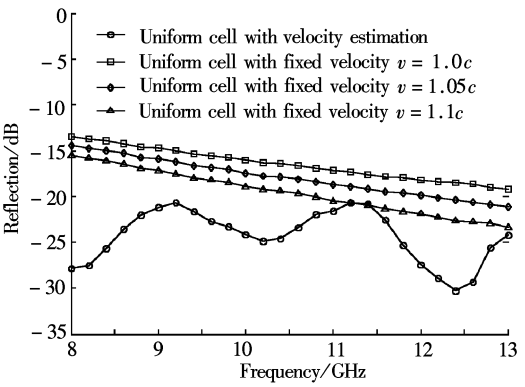

Fig. 3 Comparison of the reflection coefficients of the ABC with vs. without the velocity estimation

4.2 Nonuniform cell processing example

The performance of the ABC with nonuniform cell processing method is investigated with the parameters: $\Delta z_1 = 1$ mm, and $\Delta z_2 = 0.5$ mm.

Fig. 4 describes the comparison of the ABC with uniform cell and nonuniform cell processing. Δz in (8) becomes smaller under the nonuniform cell processing method, which diminishes the reflection of the ABC. Evident improvement can be seen in Fig. 4 with the nonuniform processing vs. the uniform one.

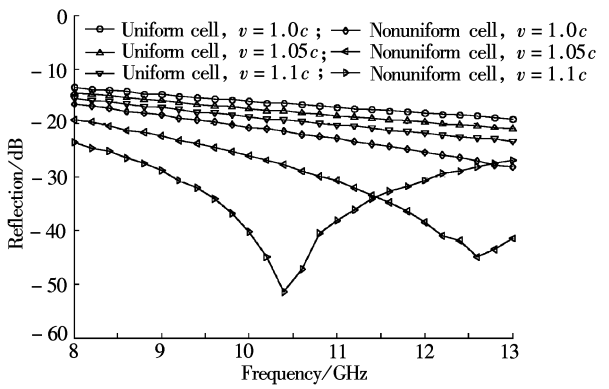

Fig. 4 Comparison of the reflection coefficients of the ABC with uniform cells vs. nonuniform cells

Fig. 5 presents different results of the nonuniform cell processing in Ref. [4] and the results in this paper. The appropriate nonuniform processing in (16) will provide a satisfying enhancement regarding the absorption of the ABC.

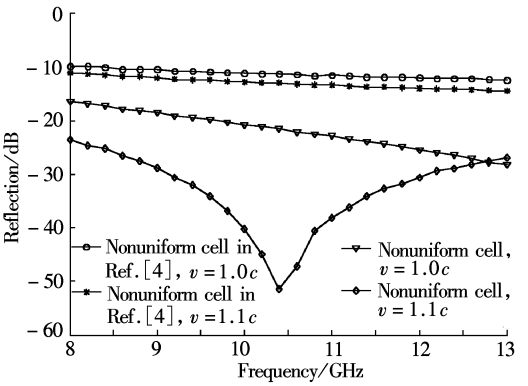

Fig. 5 Comparison of the reflection coefficients of the ABC with the nonuniform cell processing in Ref. [4] vs. the processing in this paper

4.3 Example of different time steps

As mentioned above, the performance of the ABC degrades as the time step increases. Simulations with several different time steps have also been conducted in this paper to investigate such degradation. Fig. 6 provides the reflections of the ABC with different time steps: $\Delta t = 4.7$ ps, $\Delta t = 7.05$ ps and $\Delta t = 9.4$ ps; i. e., the CFL factor (under the condition of coarse cells) is 2, 3 and 4, respectively. It should be noted that the CFL factor (under the condition of coarse cells) cannot be too great because of numerical dispersion. When the CFL factor is greater than 5, the numerical dispersion of the ADI-FDTD is unacceptable. For computation efficiency and numerical accuracy, the CFL factor (under the condition of coarse cells) is generally between 2 and 4.

Fig. 6 presents different results under different time step conditions with uniform and nonuniform cell processing respectively. From the numerical results, the reflection of the proposed ABC increases with the increase in the time step; however, the proposed ABC has quite good absorption. According to the comparison, the nonuniform cell processing provides better absorption. It also can be noted that the variation of the time step has little effect on the reflection coefficients of the ABC with uniform cell processing, which can be verified from Eq. (8). According to Eq. (8), if Δt increa-

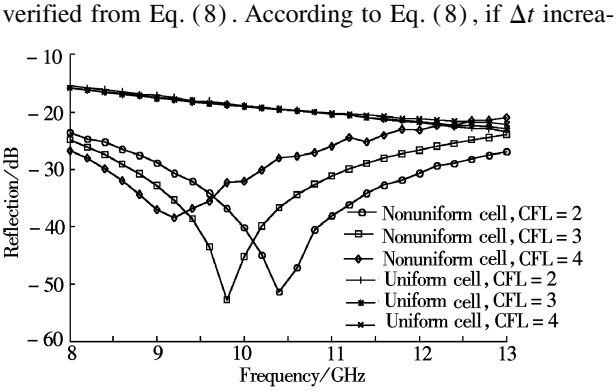

Fig. 6 Comparison of the reflection coefficients of the ABC under different time step conditions

ses, ξ will decrease correspondingly so as to keep P_{err} almost invariable.

5 Conclusion

In this paper, methods to improve the absorption of the ABC for the ADI-FDTD from two aspects are developed. One is based on the traveling wave velocity estimation to eliminate the reflection of the ABC, the other is based on the nonuniform cell processing to decrease the reflection and on the appropriate nonuniform cell processing to better describe the gradual change in the nonuniform interface. The simulation example is completed in the case of a rectangular waveguide with strong dispersive characteristics. According to the simulation results, obvious improvements of the ABC have been obtained by the two methods for the ADI-FDTD.

References

[1] Yee K S. Numerical solution of initial boundary value problems involving Maxwell's equations in isotropic media [J]. *IEEE Transactions on Antennas and Propagation*, 1966, **14**(3): 302 - 307.

[2] Taflove A, Hagness S C. *Computational electrodynamics: the finite-difference time-domain method* [M]. Boston: Artech House, 2000.

[3] Zheng F, Chen Z, Zhang J. Toward the development of a three-dimensional unconditionally stable finite-difference time-domain method [J]. *IEEE Transactions on Microwave Theory and Techniques*, 2000, **48**(9): 1550 - 1558.

[4] Namiki T. 3-D ADI-FDTD method—unconditionally stable time domain algorithm for solving full vector Maxwell's equations [J]. *IEEE Transactions on Microwave Theory and Techniques*, 2000, **48**(10): 1743 - 1748.

[5] Mur G. Absorbing boundary conditions for the finite-difference approximation of the time-domain electromagnetic field equations [J]. *IEEE Transactions on Electromagnetic Compatibility*, 1981, **23**(11): 377 - 382.

[6] Zhou J Y, Hong W. Construction of the absorbing boundary conditions for the FDTD method with transfer functions [J]. *IEEE Transactions on Microwave Theory and Techniques*, 1998, **46**(11): 1807 - 1809.

[7] Shao Z H, Hong W, Zhou J Y. Generalized *Z*-domain absorbing boundary conditions for the analysis of electromagnetic problems with finite-difference time-domain method [J]. *IEEE Transactions on Microwave Theory and Techniques*, 2003, **51**(1): 82 - 90.

[8] Berenger J P. A perfectly matched layer for absorption of electromagnetic waves [J]. *J Compu Phys*, 1994, **114**(10): 185 - 200.

[9] Wang S, Teixeira F L. An efficient PML implementation for the ADI-FDTD method [J]. *IEEE Microwave and Wireless Component Letter*, 2003, **13**(2): 72 - 74.

[10] Li J, Dai J. An efficient implementation of the stretched coordinate perfectly matched layer [J]. *IEEE Microwave and Wireless Component Letter*, 2007, **17**(5): 322 - 324.

[11] Hwang J, Chen F C. Numerical performances of absorbing boundary conditions for ADI-FDTD method [C]//*IEEE Antennas and Propagation Society International Symposium*. New Mexico, USA, 2006: 2723 - 2726.

适用于 ADI-FDTD 的基于线性插值的吸收边界条件及其改进方法

赵嘉宁

(东南大学移动通信国家重点实验室,南京 210096)

摘要:基于线性插值的方法提出了一种适用于交替方向隐式时域有限差分法(ADI-FDTD)的吸收边界条件,该边界条件能够在 ADI-FDTD 方法中改善边界反射性能. 首先,对由截断误差和相速估计误差引起的此吸收边界条件的反射进行了分析和推导. 通过理论分析,说明了基于相速估计和非均匀网格的对此吸收边界改进方法能够改善边界条件的反射特性. 然后进行了矩形波导情况下该吸收边界条件的数值仿真. 最后给出了数值仿真结果,并通过对有无相速估计下吸收边界条件反射系数比较、对均匀和非均匀网格处理下吸收边界条件反射系数的比较,以及对在不同时间步长下吸收边界条件反射系数变化的分析,说明了该吸收边界条件及其改进方法对 ADI-FDTD 方法中的边界反射性能有很好的改善效果.

关键词:交替方向隐式时域有限差分法;吸收边界条件;线性插值;相速;不均匀网格

中图分类号:O441.4;TN011